Synthesis of Rutile-Related Oxides, $LiMMoO_6$ (M = Nb, Ta), and Their Proton Derivatives. Intercalation Chemistry of Novel Bronsted Acids, $HMMoO_6 \cdot H_2O$†

N. S. P. Bhuvanesh and J. Gopalakrishnan*

Solid State and Structural Chemistry Unit, Indian Institute of Science, Bangalore 560012, India

Received February 15, 1995®

Rutile-related oxides of the formula $LiMMoO_6$ for M = Nb or Ta have been synthesized for the first time (a = 4.685(3), c = 9.25(1) Å for M = Nb and a = 4.674(1), c = 9.23(1) Å for M = Ta). These oxides undergo topochemical proton exchange in dilute HNO_3, yielding layered $HMMoO_6 \cdot H_2O$ that retain the rutile-like $MMoO_6$ slabs (a = 4.690(9), c = 26.75(8) Å for M = Nb and a = 4.687(1), c = 26.71(1) Å for M = Ta). The monohydrates undergo stepwise dehydration, yielding hemihydrates and anhydrous $HMMoO_6$. $HMMoO_6 \cdot H_2O$ are strong Bronsted acids, intercalating a wide variety of organic bases, including pyridine (pK_a = 5.3), aniline (pK_a = 4.6), and pyrrole (pK_a = 0.4).

Introduction

$LiMWO_6$ (M = Nb, Ta) crystallize in a novel trirutile structure[1,2] (space group $P\bar{4}2_1m$) where the lithium ions are ordered in layers perpendicular to the c axis. Accordingly, these materials readily exchange lithium ions with protons in aqueous acid, yielding new layered oxides,[3,4] $HMWO_6 \cdot nH_2O$, which exhibit strong Bronsted acidity.[3,5,6] Surprisingly, the corresponding molybdenum compounds have not been reported.[1] In view of the interesting properties exhibited by this class of materials (ion exchange,[3,4] luminescence, nonlinear optical response,[7] and ionic conductivity[8]), we considered it important to synthesize the molybdenum analogs of $LiMWO_6$. We have been able to synthesize the molybdenum compounds, $LiMMoO_6$, by a new synthetic procedure, which involves solid state reaction of constituent oxides with Li_2CO_3 at 580−600 °C, followed by quenching the products in air. We have also synthesized the protonated derivatives of $LiMMoO_6$ by ion exchange and investigated their Bronsted acidity by intercalation of several organic bases. Our results, which are reported in this paper, reveal that the protonated derivatives, $HMMoO_6 \cdot H_2O$, are among the strongest solid Bronsted acids known with a layered structure, intercalating a wide variety of organic bases, including the weak ones, such as pyridine (pK_a = 5.3), aniline (pK_a = 4.6), and pyrrole (pK_a = 0.4).

Experimental Section

We investigated the formation of $LiMMoO_6$ by reacting Li_2CO_3, M_2O_5 (M = Nb, Ta), and MoO_3 at various temperatures under different conditions. After several attempts, we found that single-phase $LiMMoO_6$, isostructural with $LiMWO_6$, were formed under the following conditions: solid state reaction (at 580 °C for M = Nb and 600 °C for M = Ta) for 24 h with one intermittent grinding followed by quenching the products in air.

Proton exchange of $LiMMoO_6$ was carried out by treating 1 g portions of the parent oxides in 100 mL aliquots of 2 M HNO_3 at room temperature with stirring. Lithium exchange, monitored by flame photometry, revealed that the exchange was ~98% complete at the end of 1 day and nearly 100% complete after 2 days. After exchange, the products were washed and dried in a desiccator over anhydrous $CaCl_2$.

Intercalation of n-alkylamines in $HMMoO_6 \cdot H_2O$ (M = Nb, Ta) was carried out by refluxing the solid with a 10% solution of the amine in n-heptane. Intercalation of weak organic bases with pK_a ranging from 5.3 to 0.4 was carried out either by direct reaction of the host solid with neat bases (aniline, pyridine, 4-methylaniline, 3-methylaniline, and pyrrole) at room temperature or by refluxing the host with a 10% solution of the base (4-nitroaniline and 3-nitroaniline) in ethanol.

$LiMMoO_6$ and their derivatives were characterized by powder X-ray diffraction (XRD), energy dispersive X-ray emission (EDX) analysis, and thermogravimetric (TG) analysis as described elsewhere.[9] Infrared (IR) spectra of powdered samples dispersed in KBr disks were recorded with a Bio-Rad SKC-3200 FTIR spectrometer. Lattice parameters were derived from least-squares refinement of the powder XRD data using the PROSZKI program that includes LAZY PULVERIX.[10]

Results and Discussion

Synthesis and Characterization of $LiMMoO_6$ (M = Nb, Ta). It has been reported[1b,2] that $LiMWO_6$ (M = Nb, Ta) exists in two modifications, a low-temperature trirutile modification, which is stable up to ~800 °C, and a rhombohedral $LiNbO_3$ type phase, stable above this temperature. The molybdenum analogs of the trirutile $LiMWO_6$ have not been reported so far. Since the trirutile−$LiNbO_3$ transformation for $LiMWO_6$ is irreversible, the trirutile structure for $LiMWO_6$ is most likely metastable, existing only at lower temperatures (≤800 °C). Accordingly, we anticipated that the trirutile structure for the molybdenum analogs would also be metastable. We therefore investigated the formation of molybdenum analogs by reaction of the constituent oxides and Li_2CO_3 at various temperatures <800 °C, followed by quenching or slow cooling. We found that single-phase trirutile materials corresponding to the composition $LiMMoO_6$ (M = Nb, Ta) could be stabilized by the

* Author to whom correspondence should be addressed.

† Contribution No. 1096 from the Solid State and Structural Chemistry Unit.

® Abstract published in *Advance ACS Abstracts,* June 15, 1995.

(1) (a) Viebahn, W.; Rüdorff, W.; Kornelson, H. Z. *Naturforsch.* **1967**, *22B*, 1218. (b) Blasse, G.; de Pauw, A. D. M. *J. Inorg. Nucl. Chem.* **1970**, *32*, 3960.
(2) Fourquet, J. L.; Le Bail, A.; Gillet, P. A. *Mater. Res. Bull.* **1988**, *23*, 1163.
(3) Bhat, V.; Gopalakrishnan, J. *Solid State Ionics* **1988**, *26*, 25.
(4) Kumada, N.; Horiuchi, O.; Muto, F.; Kinomura, N. *Mater. Res. Bull.* **1988**, *23*, 209.
(5) Kinomura, N.; Amano, S.; Kumada, N. *Solid State Ionics* **1990**, *37*, 317.
(6) Kinomura, N.; Kumada, N. *Solid State Ionics* **1992**, *51*, 1.
(7) Wiegel, M.; Emond, M. H. J.; de Bruin, T. H. M.; Blasse, G. *Chem. Mater.* **1994**, *6*, 973.
(8) (a) Ohtsuka, H.; Yamaji, A.; Okada, T. *Solid State Ionics* **1984**, *14*, 283. (b) Ohtsuka, H.; Okada, T. *Solid State Ionics* **1986**, *20*, 141.
(9) Gopalakrishnan, J.; Bhuvanesh, N. S. P.; Raju, A. R. *Chem. Mater.* **1994**, *6*, 373.
(10) Lasocha, W.; Lewinski, K. *J. Appl. Crystallogr.* **1994**, *27*, 437.

0020-1669/95/1334-3760$09.00/0

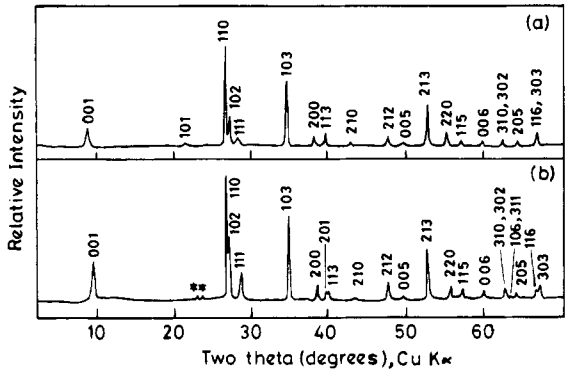

Figure 1. X-ray powder diffraction patterns of (a) $LiNbMoO_6$ and (b) $LiTaMoO_6$. Asterisks in (b) denote reflections due to $LiTaO_3$ impurity.

Table 1. X-ray Powder Diffraction Data for $LiNbMoO_6$ and $LiTaMoO_6$

	M = Nb				M = Ta			
h k l	d_{obs} (Å)	d_{cal} (Å)	I_{obs}	I_{cal}[a]	d_{obs} (Å)	d_{cal} (Å)	I_{obs}	I_{cal}[a]
0 0 1	9.56	9.25	19	66	9.40	9.23	35	67
1 0 1	4.171	4.179	4	19				
1 1 0	3.320	3.312	100	100	3.302	3.305	100	100
1 0 2	3.273	3.291	33	55	3.273	3.283	52	58
1 1 1	3.137	3.118	10	16	3.116	3.111	20	18
1 0 3	2.578	2.576	66	63	2.571	2.568	69	70
2 0 0	2.344	2.343	10	13	2.335	2.337	14	18
2 0 1					2.265	2.265	8	6
1 1 3	2.259	2.257	10	10	2.251	2.251	8	6
2 1 0	2.103	2.095	4	3	2.090	2.090	2	2
2 1 2	1.907	1.908	10	20	1.901	1.904	15	21
0 0 5	1.838	1.850	4	4	1.843	1.845	4	4
2 1 3	1.737	1.733	43	58	1.729	1.729	46	57
2 2 0	1.663	1.656	15	18	1.653	1.653	13	17
1 1 5	1.608	1.615	7	11	1.610	1.611	9	12
0 0 6	1.543	1.542	6	5	1.542	1.537	6	5
3 1 0		1.482		12		1.478		13
	1.486		8		1.479		10	
3 0 2		1.480		4		1.476		4
1 0 6					1.460		1	
					1.462		3	
3 1 1						1.459		3
2 0 5	1.447	1.452	6	8	1.447	1.448	6	8
1 1 6		1.398		17	1.397	1.397	8	10
	1.397		16					
3 0 3		1.393		19	1.390	1.390	11	16
	$a = 4.685(3)$, $c = 9.25(1)$ Å				$a = 4.674(1)$, $c = 9.23(1)$ Å			

[a] Calculated by the LAZY PULVERIX program using the positional parameters[2] of $LiNbWO_6$.

reaction at 580 °C for M = Nb and at 600 °C for M = Ta, followed by quenching the products in air. Reaction at temperatures higher than 610 °C for M = Nb yields multiphasic materials consisting mainly of $LiNbO_3$ and $LiNb_3O_8$ type phases.

XRD patterns of $LiMMoO_6$ (Figure 1) are indexable (Table 1) on tetragonal cells with $a = 4.685(3)$, $c = 9.25(1)$ Å for M = Nb and $a = 4.674(1)$, $c = 9.23(1)$ Å for M = Ta. Both the patterns and the unit cell parameters are closely similar to those of the corresponding trirutile $LiMWO_6$ phases[3] ($a = 4.681(6)$, $c = 9.28(1)$ Å for M = Nb and $a = 4.669(3)$, $c = 9.301(6)$ Å for M = Ta). We see in $LiMMoO_6$ a small increase in the a parameter and a decrease in the c parameter. There is an overall decrease in the cell volume of $LiMMoO_6$ as compared to the volume of $LiMWO_6$, which is consistent with the ionic radii of Mo(VI) and W(VI) (0.59 and 0.60 Å respectively). $LiNbWO_6$ crystallizes in a tetragonal structure,[2] space group $P\bar{4}2_1m$, where Li, Nb, and W atoms are ordered in layers perpendicular to the c direction. There is a 10% disorder between Nb and W atoms in this structure.[2] In an attempt to show that $LiMMoO_6$ are

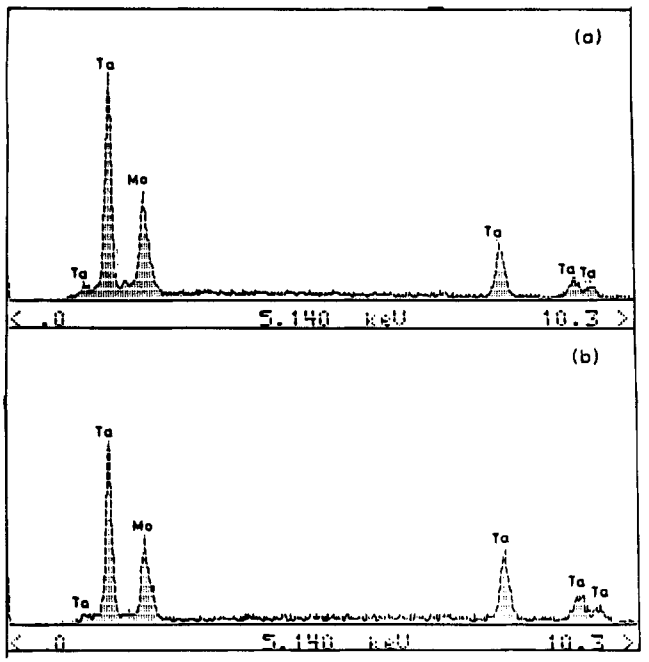

Figure 2. EDX spectra of (a) $LiTaMoO_6$ and (b) $HTaMoO_6{\cdot}H_2O$.

isostructural with $LiMWO_6$, we calculated the XRD intensities of $LiTaMoO_6$ using the position parameters[2] of $LiNbWO_6$, for various distributions of cations. A satisfactory agreement between the observed and calculated intensities is obtained for a model where Li atoms are ordered at 2*c* (0, 1/2, 0.420) sites and Mo and Ta are randomly distributed at 2*c* (0, 1/2, 0.0901; 0, 1/2, 0.7305) sites in the space group $P\bar{4}2_1m$. A similar calculation of the intensities for $LiNbMoO_6$ could not distinguish between ordered and disordered models, because the mean atomic scattering factors of both Mo and Nb are similar. From powder XRD data, we therefore believe that both $LiNbMoO_6$ and $LiTaMoO_6$ are grossly isostructural with the corresponding tungsten analogs, although the exact details of ordering of M/Mo and M/W atoms in the two sets of oxides is most likely dependent on the synthesis conditions.

Synthesis and Characterization of Layered $HMMoO_6{\cdot}nH_2O$. Since $LiMWO_6$ undergo proton exchange[3,4] in aqueous acids to give layered $HMWO_6{\cdot}nH_2O$, we expected that $LiMMoO_6$ also would undergo a similar exchange, forming layered $HMMoO_6{\cdot}nH_2O$. Indeed, we could readily prepare hydrated $HMMoO_6$ by treating $LiMMoO_6$ with 2 M HNO_3 for 2 days at room temperature. We examined the ion-exchanged product of the tantalum compound by EDX analysis to establish the composition. The results (Figure 2) show that the Ta:Mo ratio remains 1:1 in the protonated material as in the parent $LiTaMoO_6$, indicating that only lithium ions are exchanged during the acid treatment. TG analyses (Figure 3) show that the protonated phases are monohydrates, $HMMoO_6{\cdot}H_2O$, losing the water of hydration and forming anhydrous $HMMoO_6$ at ~230 °C. TG data indiate the formation of a hemihydrate around 120 °C, but it is difficult to isolate it because of its tendency to rehydrate easily. XRD patterns (Figure 4) show that the monohydrates (Table 2) and the anhydrous phases crystallize in tetragonal structures (Table 3), derived from the parent $LiMMoO_6$. While the a parameter (~4.69 Å) of $HMMoO_6{\cdot}H_2O$ remains nearly the same as that of the parent $LiMMoO_6$, the value of the c parameter (~26.7 Å) indicates not only an expansion of the lattice due to hydration but also a doubling as well in this direction. On dehydration, the c parameter decreases by ~5.5 Å in $HMMoO_6$, but the lattice doubling remains. More interestingly, the proton exchange is accompanied by a transforma-

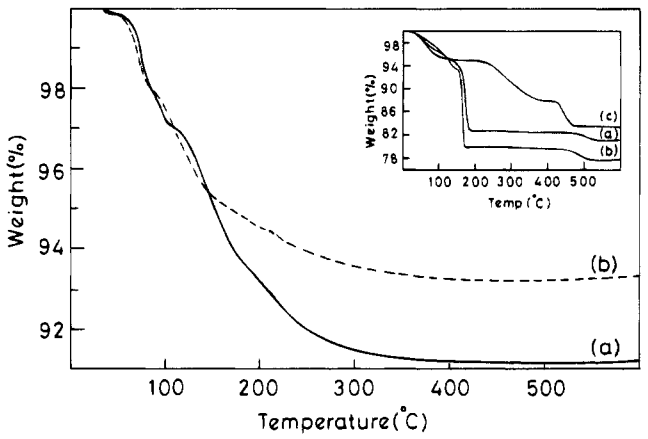

Figure 3. Thermogravimetric (TG) curves of (a) $HNbMoO_6 \cdot H_2O$ and (b) $HTaMoO_6 \cdot H_2O$. In the inset are shown TG curves of intercalation compounds of $HNbMoO_6 \cdot H_2O$ with (a) *n*-butylamine, (b) *n*-hexylamine, and (c) aniline. TG curves (inset) were recorded at a heating rate of 2 °C/min in a flowing oxygen atmosphere.

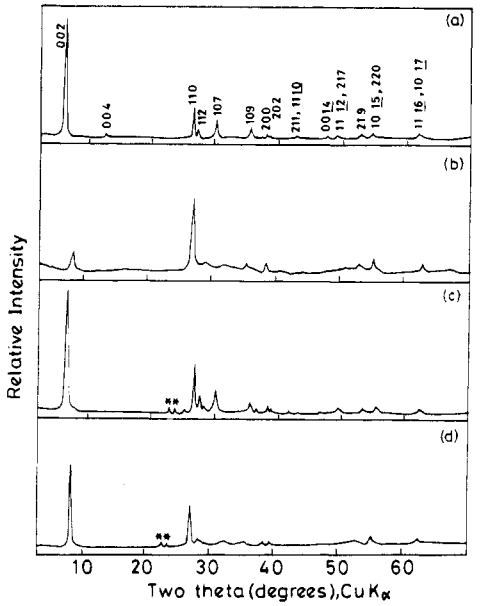

Figure 4. X-ray powder diffraction patterns of (a) $HNbMoO_6 \cdot H_2O$, (b) $HNbMoO_6$, (c) $HTaMoO_6 \cdot H_2O$, and (d) $HTaMoO_6$. Asterisks in (c) and (d) denote reflections due to $LiTaO_3$ impurity present in the parent $LiTaMoO_6$ preparation.

tion of the lattice from primitive to body-centered tetragonal, as revealed by the XRD patterns of $HMMoO_6 \cdot H_2O$ (Figure 4; Table 2). These structural changes most likely indicate a displacement of the adjacent $MMoO_6$ slabs by the translation $(a + b)/2$, in the protonated phases. A similar structural change occurs in the tungsten analogs of $HMMoO_6$ as well as in $HCa_2Nb_3O_{10}$ during their formation by ion exchange.[3,11] A schematic representation of the idealized structures of $LiMMoO_6$, $HMMoO_6 \cdot H_2O$, and anhydrous $HMMoO_6$ is shown in Figure 5. The presence of characteristic absorption bands[12] of H_3O^+ at 3375, 1620, and 1105 cm^{-1} in the IR spectrum of $HNbMoO_6 \cdot H_2O$ suggests that the intercalated water in $HMMoO_6 \cdot H_2O$ most likely exists as H_3O^+. Accordingly, the monohydrates should be formulated as H_3OMMoO_6, similar to the corresponding ammonium derivatives,[13] NH_4MMoO_6.

(11) Jacobson, A. J.; Lewandowski, J. T.; Johnson, J. W. *J. Less-Common Met.* **1986**, *116*, 137.
(12) (a) Gillard, R. D.; Wilkinson, G. *J. Chem. Soc.* **1964**, 1640. (b) Nakamoto, K. *Infrared Spectra of Inorganic and Coordination Compounds*, 3rd ed.; Wiley: New York, 1978; p 119.

Table 2. X-ray Powder Diffraction Data for $HNbMoO_6 \cdot H_2O$

h k l	d_{obs} (Å)	d_{cal} (Å)	I_{obs}
0 0 2	13.09	13.37	100
0 0 4	6.697	6.689	3
1 1 0	3.326	3.316	26
1 1 2	3.226	3.218	9
1 0 7	2.959	2.962	16
1 0 9	2.518	2.510	9
2 0 0	2.356	2.345	4
2 0 2	2.320	2.309	2
2 1 1	2.099	2.091	2
1 1 10		2.082	
0 0 14	1.897	1.910	2
1 1 12	1.845	1.850	3
2 1 7		1.838	
2 1 9	1.719	1.713	3
1 0 15	1.664	1.667	5
2 2 0		1.658	
1 1 16	1.489	1.492	5
1 0 17		1.492	

$a = 4.690(9)$, $c = 26.75(8)$ Å

Table 3. Composition and Lattice Parameters of $LiMMoO_6$, $HMMoO_6 \cdot H_2O$, and Anhydrous $HMMoO_6$ (M = Nb, Ta)

	lattice params (Å)	
compn	*a*	*c*
$LiNbMoO_6$	4.685(3)	9.25(1)
$LiTaMoO_6$	4.674(1)	9.23(1)
$HNbMoO_6 \cdot H_2O$	4.690(9)	26.75(8)
$HNbMoO_6$	4.694(5)	21.34(2)
$HTaMoO_6 \cdot H_2O$	4.687(1)	26.71(1)
$HTaMoO_6$	4.672(1)	21.04(1)

Bronsted Acidity of $HMMoO_6 \cdot H_2O$. It is known[3,5,6] that $HMWO_6$ (M = Nb, Ta) and their hydrates are strong Bronsted acids, intercalating a wide variety of organic bases. We anticipated that the analogous $HMMoO_6$ would also be strong Bronsted acids. Accordingly, we investigated the Bronsted acidity of the molybdenum compounds by intercalating several organic bases in $HNbMoO_6 \cdot H_2O$. *n*-Alkylamines, for instance, react readily with $HNbMoO_6 \cdot H_2O$, forming intercalation compounds with large expansions of the *c* axis (Figure 6; Table 4). TG analysis shows that the water of hydration is retained in the intercalation compounds. The amine contents, determined by the weight losses in TG experiments (Figure 3 inset), are ~0.5 mol/mol of the host solid (Table 4). Similar results have been reported[5] for the *n*-alkylamine intercalation compounds of $HTaWO_6 \cdot 0.5H_2O$.

A plot of the *c* parameter of the *n*-alkylamine intercalation compounds of $HNbMoO_6 \cdot H_2O$ with the number (*n*) of carbon atoms in the amine (Figure 7) shows a linear relation that fits into the equation $c = 1.96n + 13.17$ Å. Assuming that the alkyl chains are in the *all-trans* conformation, a slope of 1.96 Å indicates a bilayer arrangement of the alkyl chains.[14] The chains are inclined at an angle $\alpha = 50.5°$, $\sin^{-1}(1.96/2 \times 1.27)$, with respect to the inorganic layer surface. The intercept of 13.17 Å is slightly larger than the basal spacing (12.20 Å) of the ammonium derivative[13] NH_4NbMoO_6. A direct comparison of the intercept with the basal spacing of the ammonium

(13) NH_4NbMoO_6 was prepared by treating $HNbMoO_6 \cdot H_2O$ with molten NH_4NO_3 at 180 °C for 3 days, followed by washing with distilled water and drying the solid over anhydrous $CaCl_2$. It crystallizes in a tetragonal structure ($a = 4.69(3)$, $c = 12.20(4)$ Å) related to the host.
(14) (a) Jacobson, A. J.; Johnson, J. W.; Lewandowski, J. T. *Mater. Res. Bull.* **1987**, *22*, 45. (b) Cao, G.; Mallouk, T. E. *Inorg. Chem.* **1991**, *30*, 1434.

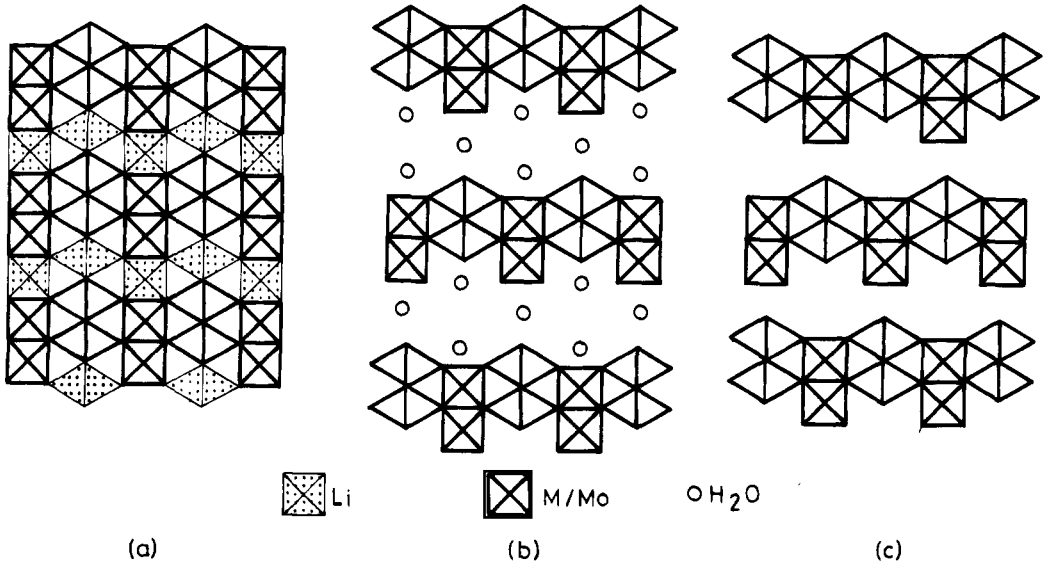

Figure 5. Schematic representation of the structures of (a) rutile-type $LiMMoO_6$, (b) $HMMoO_6 \cdot H_2O$, and (c) $HMMoO_6$ (M = Nb, Ta).

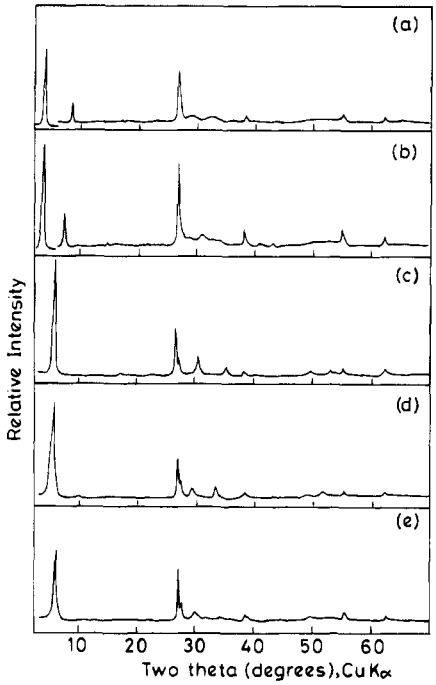

Figure 6. X-ray powder diffraction patterns of typical intercalation compounds of $HNbMoO_6 \cdot H_2O$ with (a) *n*-butylamine, (b) *n*-hexylamine, (c) pyridine, (d) aniline, and (e) pyrrole.

derivative is however inappropriate, because the *n*-alkylamine intercalation compounds retain the water of hydration of the host, while the ammonium derivative is anhydrous. All the *n*-alkylamine intercalation compounds of $HNbMoO_6 \cdot H_2O$ undergo partial dehydration on drying around 100 °C in a vacuum oven (pressure $\sim 10^{-1}$ Torr), resulting in a decrease in the basal spacing (e.g., *c* decreases from 24.5 to 22.1 Å, 27.1 to 24.5 Å, and 36.5 to 33.8 Å, respectively, for *n*-hexyl-, *n*-heptyl-, and *n*-dodecylamine intercalates). The decrease (~2.5 Å) corresponds approximately to the diameter of a water molecule[15] (2.8 Å). It is therefore likely that, in the *n*-alkylamine intercalation compounds of $HNbMoO_6 \cdot H_2O$, the water molecules separate the *n*-alkylamines from the inorganic host layer.[16] Significantly, the intercalates rehydrate on exposure to atmosphere with concomitant increase in the *c* parameter to its original value.

(15) Beneke, K.; Lagaly, G. *Inorg. Chem.* **1987**, *26*, 2537.
(16) This was suggested by one of the reviewers of this paper.

Table 4. Composition and Lattice Parameters of Intercalation Compounds of $HMMoO_6 \cdot H_2O$ (M = Nb, Ta) with *n*-Alkylamines

n-alkylamine	intercalated amine content[a]	lattice params (Å)	
		a	*c*
n-butylamine	0.47	4.70	20.9
n-pentylamine	0.54	4.70	23.0
n-hexylamine	0.51	4.70	24.5
n-heptylamine	0.48	4.72	27.1
n-octylamine	0.53	4.72	29.4
n-nonylamine	0.53	4.71	30.9
n-decylamine	0.57	4.73	32.8
n-dodecylamine	0.61	4.71	36.5
n-hexylamine[b]	0.51	4.69	24.2

[a] Denotes number of formula units of amine intercalated per formula unit of $HMMoO_6H_2O$. [b] The host in this case is $HTaMoO_6 \cdot H_2O$. In all other cases, the host is $HNbMoO_6 \cdot H_2O$.

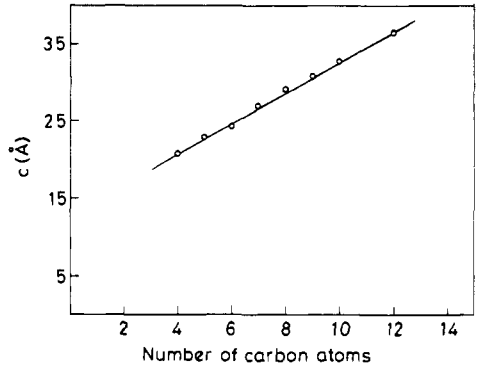

Figure 7. Plot of *c* parameter versus number of carbon atoms in the *n*-alkylamine intercalation compounds of $HNbMoO_6 \cdot H_2O$.

The acid–base intercalation reaction between $HNbMoO_6 \cdot H_2O$ and *n*-alkylamines is incomplete, as revealed by the intercalated amine content; only about 0.5 mol of amine is intercalated by 1 mol of the host (Table 4). The guest:host ratio of ~0.5 suggests two different possibilities: (1) the intercalation compounds are stage 2 derivatives (i.e., the guest molecules intercalate at all the acid sites between alternate layers) or (2) the guest molecules intercalate uniformly between all the layers, making use of approximately half the acid sites in every layer. Formation of stage 2 intercalates appears unlikely on the basis of geometric (steric) considerations: the cross-sectional area[17] of an *n*-alkyl chain in the *all-trans* conformation is ~19.3 $Å^2$, whereas the area per acid site in $HNbMoO_6 \cdot H_2O$ is ~11 $Å^2$.

Table 5. Composition and Lattice Parameters of Intercalation Compounds of $HMMoO_6 \cdot H_2O$ (M = Nb, Ta) with Weak Organic Bases

guest	pK_a	guest:host ratio	c^a (Å)	Δc^b (Å)
pyridine	5.3	0.20	15.6	4.9
aniline	4.6	0.31	17.6	6.9
4-methylaniline	5.1	0.40	20.2	9.5
3-methylaniline	4.7	0.38	20.9	10.2
4-nitroaniline	1.0	0.26	19.7	9.0
3-nitroaniline	2.5	0.15	21.8	11.1
pyrrole	0.4	0.25	15.5	4.8
pyridine[c]	5.3	0.20	15.2	5.2
pyrrole[c]	0.4	0.33	15.5	4.8

[a] The *a* parameter of the intercalates is ~4.70 Å in all cases. [b] The lattice expansion is given with respect to anhydrous $HNbMoO_6$/$HTaMoO_6$. [c] The host in these cases is $HTaMoO_6 \cdot H_2O$. In all other cases, the host is $HNbMoO_6 \cdot H_2O$.

Therefore, intercalating *n*-alkylamines at *all* the acid sites in a layer of $HNbMoO_6 \cdot H_2O$ is sterically impossible, ruling out stage 2 intercalation. If, on the other hand, we assume that intercalation occurs uniformly between every layer, the limiting guest:host ratio expected on the basis of geometric considerations is 11.0:19.3 = 0.57. The experimentally found guest:host ratios of the *n*-alkylamine intercalation compounds (Table 4) are therefore consistent with the uniform intercalation model.

The high-density of acid sites (11 $Å^2$ per site) in $HNbMoO_6 \cdot H_2O$ is comparable to the exchange site densities[18] of brittle micas (12 $Å^2$) and $KNiAsO_4$ (10.8 $Å^2$). Brittle micas do not undergo ready exchange with organic cations, but $KNiAsO_4$ does undergo[18] exchange with alkylammonium ions to an extent of about 60%.

We have investigated the intercalation of several weak organic bases such as pyridine, aniline, and pyrrole in $HNbMoO_6 \cdot H_2O$. From the TG data (Table 5), we see that the guest:host ratio in all the cases is ~0.2–0.4, indicating incomplete reaction. The expansion (Table 5) of the lattice in the *c* direction with respect to anhydrous $HNbMoO_6$ ranges from ~5.0 to ~11.0 Å, depending on the dimension as well as the quantity of the base intercalated. Typically, lattice expansions of ~5.0 Å in the case of pyridine and ~6.9 Å in the case of aniline are consistent with a perpendicular orientation of these organic bases in the interlayer space. Similar lattice expansions have been reported for $VOPO_4$–pyridine[19] (5.5 Å) and MoO_3–aniline[20] (6.7 Å) intercalates. The IR spectrum of the aniline intercalate (Figure 8) shows a sharp absorption band at 1490 cm^{-1}, indicating the formation of anilinium ions[21] due to the acid–base interaction with protons of $HNbMoO_6 \cdot H_2O$. The pyridine intercalate also behaves similarly, showing an absorption band at 1535 cm^{-1}, which is characteristic of the pyridinium ion.[6,19]

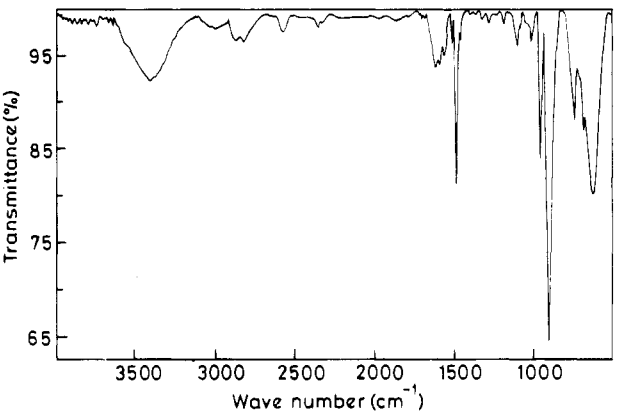

Figure 8. Infrared spectrum of $(C_6H_5NH_3)_{0.3}H_{0.7}NbMoO_6 \cdot H_2O$.

Intercalation of a few typical organic bases (*n*-alkylamines and pyridine) in $HTaMoO_6 \cdot H_2O$ reveals that the Bronsted acidity of this oxide is similar to that of $HNbMoO_6 \cdot H_2O$ (Tables 4 and 5). More interestingly, both $HNbMoO_6 \cdot H_2O$ and $HTaMoO_6 \cdot H_2O$ react with pyrrole (pK_a = 0.4), forming intercalation compounds of composition $(pyrrole)_yHMMoO_6 \cdot H_2O$ (y = 0.25 for M = Nb and y = 0.33 for M = Ta) (Table 5). The *c* parameter increases by ~4.80 Å in both pyrrole intercalates; the lattice expansion is of the same order as the expansions of polypyrrole-intercalated FeOCl (5.23 Å)[22] and fluorohectorite (4.55 Å).[23] $HTaWO_6 \cdot 0.5H_2O$ has been reported[6] to intercalate weak bases such as quinoxaline (pK_a = 0.56) and pyrazine (pK_a = 0.65) but does not intercalate pyrrole. We therefore believe that both $HNbMoO_6 \cdot H_2O$ and $HTaMoO_6 \cdot H_2O$ are among the strongest solid Bronsted acids consisting of metal–oxygen octahedra.[6,14a,24]

Acknowledgment. We thank Professor C. N. R. Rao for valuable encouragement and support. Our thanks are also due to Mr. A. R. Raju, Materials Research Center of this institute, for recording the EDX spectra and the Department of Science and Technology, Government of India, for financial support. N.S.P.B. thanks the Council of Scientific and Industrial Research, New Delhi, for the award of a senior research fellowship.

IC950171I

(17) Choy, J. H.; Noh, D. Y.; Park, J. C.; Chang, S. H.; Delmas, C.; Hagenmuller, P. *Mater. Res. Bull.* **1988**, *23*, 73.
(18) Beneke, K.; Lagaly, G. *Clay Miner.* **1982**, *17*, 175.
(19) Johnson, J. W.; Jacobson, A. J.; Brody, J. F.; Rich, S. M. *Inorg. Chem.* **1982**, *21*, 3820.
(20) Bissessur, R.; De Groot, D. C.; Schindler, J. L.; Kannewurf, C. R.; Kanatzidis, M. G. *J. Chem. Soc., Chem. Commun.* **1993**, 687.
(21) Bein, T.; Enzel, P. *Synth. Met.* **1989**, *29*, E163.
(22) Kanatzidis, M. G.; Tonge, L. M.; Marks, T. J.; Marcy, H. O.; Kannewurf, C. R. *J. Am. Chem. Soc.* **1987**, *109*, 3797.
(23) Mehrotra, V.; Gianellis, E. P. *Solid State Ionics* **1992**, *51*, 115.
(24) (a) Rebbah, H.; Borel, M. M.; Raveau, B. *Mater. Res. Bull.* **1980**, *15*, 317. (b) Nedjar, R.; Borel, M. M.; Raveau, B. *Z. Anorg. Allg. Chem.* **1986**, *540*, 198.